A highly thermal and pH stable fluorescence sensor for Hg^{2+}, Fe^{3+} and tetracycline in aqueous solution

Xuancheng Sun,‡[a] Chaoxiong Li,‡[a] Xianggao Meng,*[b] Dunjia Wang[a] and Chunyang Zheng*[a]

[a] Hubei Key Laboratory of Pollutant Analysis and Reuse Technology, College of Chemistry and Chemical Engineering, Hubei Normal University, Huangshi 435002, P. R. China.

[b] College of Chemistry, Central China Normal University, Wuhan 430079, P. R. China.

* E-mail: mengxianggao@ccnu.edu.cn; cyzheng@hbnu.edu.cn

CONTENTS

Materials and methods

With the exception of bbimc, all solvents and materials were purchased without any purification. UV-vis absorption analysis was performed on a U-3010 spectrophotometer at room temperature. IR spectra of the two compounds were performed on a Bruker AXS TENSOR-27 FT-IR spectrometer (FTIR) with pressed KBr pellets in the range of 4000–400 cm^{-1}. Thermogravimetric analysis was carried out with a NETZSCH STA 449F5 (TG/DTA) thermal analyzer under nitrogen flow. Powder X-ray diffraction (XRD) were performed on Bruker D2 PHASER diffractometer with Cu-*Kα* radiation (λ= 1.54186 Å). Fluorescence measurements were carried out on an F4700 (Hitachi) fluorescence spectrophotometer at room temperature.

Synthesis of ligand bbimc

A flame-dried Schlenk flask was charged with A mixture of 3,6-dibrom-9-methyl-carbazol (3.41 g, 10 mmol), benzimidazole (5.90 g, 50 mmol), K_2CO_3 (10.00 g, 72 mmol), CuI (0.44 g, 2.3 mmol) and DMF(100 mL) at room temperature under nitrogen. After being heated at 140 ºC for 72 h, the mixture was evaporated under vacuum. Thereafter, 100 mL of distilled water was added to facilitate the workup. The mixture was extracted three times with CH_2Cl_2 (100 mL), then the organic phase was further washed with distilled water and dried with anhydrous $MgSO_4$. After the filtration and evaporation, the resulting residue was purified by flash column chromatography on silica gel eluting with CH_2Cl_2/MeOH (10: 1) to give bbimc as a pale solid. Isolated yield: 2.6 g (63 %). ^{1}H NMR (300 MHz, DMSO-d_6): δ 4.04 (s, 3H), 7.31 (s, 4H), 7.61-7.78 (m, 8H), 8.62 (s, 4H) ppm; ^{13}C NMR (75.4 MHz, $CDCl_3$): δ 29.5, 110.6, 110.7, 116.9, 119.8, 122.2, 122.8, 127.9, 134.1, 140.4, 143.7 ppm. HRMS (ESI) m/z calcd for $C_{27}H_{20}N_5$ ($[M + H]^+$): 414.1719; found: 414.1711. Colorless block crystals of bmima were obtained by recrystallization in the mixed solvent of CH_2Cl_2 and CH_3OH. The detailed crystal data and structure refinement parameters are shown in Table 1.

Crystallographic studies

Single-crystal X-ray diffraction data of **1** and bbimc were collected on a Bruker APEX-II CCD or Rigaku XtaLAB Synergy-I with ω-scan pattern and Ga-K*α* radiation (λ = 1.34139 Å) or Cu Kα radiation (λ = 1.54178 Å). The diffraction profiles were integrated using the SAINT program.[S1] The structures were solved with direct methods (SHELX),[S2, S3] and refined by fullmatrix least squares on F^2 using OLEX3,[S4] which utilizes the SHELXL-2018 module. The hydrogen atoms were placed geometrically. All non-hydrogen atoms were refined anisotropically. The H atoms were generated from the computed positions and subjected to isotropic refinement. The relevant crystallographic data are summarized in Table 1. The chosen bond lengths as well as angles are presented in Table S2.

Fluorescence measurements

Well-ground powder of **1** (2 mg) was suspended in deionized H_2O (2 mL) using ultrasound for 30 min. For each sensing experiment, a 0.2 M aqueous solution of $M(NO_3)_n$ (M^{n+} = K^+, Na^+, Zn^{2+}, Cd^{2+}, Mn^{2+}, Hg^{2+}, Ag^+, Co^{2+}, Ni^{2+}, Mg^{2+}, Cu^{2+}, Pb^{2+}, Al^{3+}, Cr^{3+}, Fe^{3+}) solutions was prepared and titrated into the suspension of **1** at ambient temperature. Then, the fluorescence emission intensities of different metal ions in the mixed solvent system were measured. The anti-jamming capability of **1** were verified by competitive experiments by adding various other cations (0.2 mM) into**1** (2 mg) with a Fe^{3+} or Hg (0.2 mM) suspension in 2 mL H_2O after sonication.

The antibiotics incorporated **1** emulsions were prepared by introducing 2 mg of **1** powder into 2 mL of sodium salts aqueous solution of CTC, TC, ODZ, RDZ, MDZ, DTZ, SMZ, SDZ, STZ, CAP, CPF and LOF at a concentration of 0.2 mM. For sensing properties with respect to Fe^{3+}, 2 mg of **1** powder was added into 2.00 mL of CTC or TC aqueous solution with different concentrations. The finely ground powder of complex **1** is dispersed well in the solution, which enables substrates to be closely adhered to the surface of the MOF particles and facilitates possible host–guest interactions. To obtain the luminescent spectra, the emulsions were treated by ultrasonic treatment for 30 min to form stable emulsions before fluorescence study. Each PL emission spectra were measured at least three times and the emission intensities were found basically unvaried.

Table S1 Selected bond distances (Å) and angles (º) for **1**

1			
Cd1-O1	2.3614(14)	Cd1-O2$^{\#1}$	2.4307(13)
Cd1-O1$^{\#1}$	2.4407(14)	Cd1-O3	2.5614(17)
Cd1-O4	2.3231(15)	Cd1-N1$^{\#2}$	2.2970(17)
Cd1-N5$^{\#2}$	2.2995(18		
O1-Cd1-O1$^{\#1}$	72.39(5)	O1-Cd1-O2$^{\#1}$	125.80(5)
O1-Cd1-O3	99.94(5)	O2$^{\#1}$-Cd1-O3	132.98(5)
O1$^{\#1}$-Cd1-O3	166.37(6)	O4-Cd1-O1$^{\#1}$	136.79(5)
O2$^{\#1}$-Cd1-O1$^{\#1}$	53.71(4)	O4-Cd1-O1	149.42(5)
O4-Cd1-O2$^{\#1}$	83.97(5)	O4-Cd1-O3	53.38(6)
N1-Cd1-O1	89.95(5)	N1-Cd1-O1$^{\#1}$	85.42(5)
N1-Cd1-O2$^{\#1}$	86.20(5)	N1-Cd1-O3	83.29(5)
N1-Cd1-O4	99.98(5)	N1-Cd1-N5$^{\#2}$	70.56(6)
Symmetry codes: #1: 3/2-*x*, 3/2-*y*, 1-*z* #2: 1/2+*x*, 3/2-*y*, 1/2+*z*			

Table S2 SHAPE analysis of the Cd^{II} ions in **1**

name	ions	label	shape	symmetry	distortion(τ)
		HP-7	Heptagon	D_{7h}	30.483
		HPY-7	Hexagonal pyramid	C_{6v}	19.827
		PBPY-7	Pentagonal bipyramid	D_{5h}	**3.525**
		COC-7	Capped octahedron	C_{3v}	6.951
1	Cd1	CTPR-7	Capped trigonal prism	C_{2v}	5.253
		JPBPY-7	Johnson pentagonal bipyramid J13	D_{5h}	6.460
		JETPY-7	Johnson elongated triangular pyramid J7	C_{3v}	17.126

Table S3 Structure of 12 antibiotics

Name	Structure	Name	Structure
Chlortetracycline **CTC**	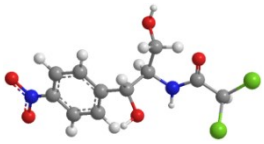	Dimetridazole **DTZ**	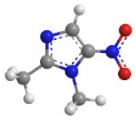
Tetracycline **TC**	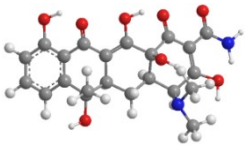	Sulfadiazine **SDZ**	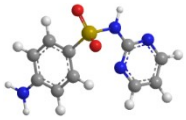
Ornidazole **ODZ**	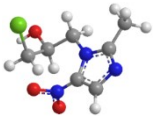	Sulfamethazine **SMZ**	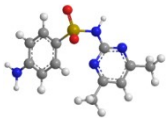
Ronidazole **RDZ**	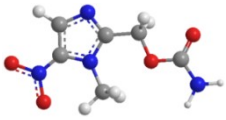	Sulfathiazole **STZ**	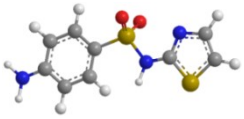
Metronidazole **MDZ**	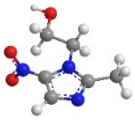	Chloramphenicol **CAP**	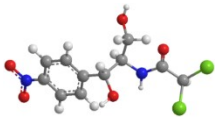
Ciprofloxacin **CPF**		levofloxacin **LOF**	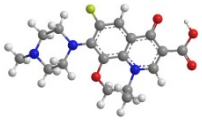

Table S4 Comparison of CP **1** with recent LCPs-based luminescent sensors for Fe^{3+}

LCPs-based chemosensor	*K*sv / M^{-1}	LOD μM	Medium	Ref.
$[Eu(BCB)(DMF)]\cdot(DMF)1.5(H_2O)_2$	4.7×10^4	0.415	H_2O	S5
{[Zn(BIBT)(oba)]·DMA}n	3.27×10^4	0.056	EtOH	S6
$\{[Cd_2(L)(1,4\text{-}NDC)_2]\cdot EtOH\}$	1.94×10^4	NR	H_2O	S7
$\{[Zn(L)\text{-}(dcdps)]\}_n$ $\{Zn(L)(bdc)\}_n$ $\{Zn(L)(bdc)\}_n$ $\{[Cd(L)(bdc)\cdot2H_2O]\cdot2DMF\}_n$	7.004×10^3 9.066×10^3 4.984×10^3 6.387×10^3	NR	H_2O	S8
Cd-DTA Zn-DTA	8.4×10^3 6.24×10^3	0.82 1.07	H_2O	S9
$[Tb(tftba)_{1.5}(phen)(H_2O)]_n$	4.043×10^4	12.7	H_2O	S10
$[In_5(TCA)_2(HTCA)_2(OH)_5]\cdot6DMF\cdot H_2O$	313907	0.382	H_2O	S11
$[Zn(H_2L)(2,2\text{-}bipy)]_n$	1.61×10^4	0.708	H_2O	S12
$\{[Eu(L_2)(H_2O)(DMF)]_n$ $[Tb(L_2)(H_2O)(DMF)]_n$	3.10×10^4 2.89×10^4	1.57 0.91	H_2O H_2O	S13
$\{[Zn_4(\mu_3\text{-}OH)_2(BTC)_2(BBI_4PY)_2]\cdot10H_2O\}_n$	3.93×10^4	0.90	H_2O	S14
$[Cd(bbimc)(ata)]_n$	**3.510×10^4**	**0.342**	**H_2O**	**This work**

Table S5 Comparison of **1** with recent LCPs-based luminescent sensors for Hg^{2+}

LCPs-based chemosensor	*K*sv / M^{-1}	LOD	Medium	Ref.
$[Zn(\mu_2\text{-}1H\text{-ade})(\mu_2\text{-}SO_4)]_n$	0.77×10^4	0.07 μM	H_2O	S15
$[Zn_2(bbmb)_2(tdc)_2]\cdot2H_2O$	48.1×10^4	0.19 μM	H_2O	S16
$Cd_3(C_{10}H_4O_7N_1)_2(H_2O)_8]$ $0.733(O_2)\cdot2(H_{1.47}O_{0.27})$	11.4×10^4	5.4 ppb	H_2O	S17
$\{[Cd_{1.5}(C_{18}H_{10}O_{10})]\cdot(H_3O)(H_2O)_3\}n$	0.43×10^4	NR	H_2O	S18
Eu^{3+}@UIO-66(DPA)	137×10^4	8.26 nM	H_2O	S19
$[Zn(2\text{-}NH_2bdc)(bibp)]n$	655×10^4	4.2×10^{-8} M	H_2O	S20
$\{[Cd(BIBT)(TDC)]\cdot2H_2O\}n$	5.05×10^4	0.097 μM	H_2O	S21
[Cd(L)(NTA)]n	0.357×10^4	3.05 μM	H_2O	S22
[Ni(L)(NPTA) H_2O]n	0.743×10^4	2.29 μM		
$\{[Cd(BIPA)(tfbdc)(H_2O)]\cdot DMF\}n$	1.27×10^4	0.12 μM	H_2O	S23
$[Co(NPDC)(bpee)]\cdot DMF\cdot2H_2O$	0.426×10^4	4.1 μM	H_2O	S24
$[Cd(bbimc)(ata)]_n$	**5.131×10^4**	**0.246 μM**	**H_2O**	**this work**

Table S6 Comparison of **1** with recent LCPs-based luminescent sensors for CTC and TC

LCPs-based chemosensor	Analyst	*K*sv / M^{-1}	LOD	Medium	Ref.
$Cu_4I_4(EBT)_5$	TC	3.8×10^2	4.8 ppm	H_2O	S25
$Cu_4I_4(ETBT)_4$	TC	3.23×10^3	4.15 μM	H_2O	S26
$(H_2bpy)_{0.5}[(UO_2)_{1.5}(ipa)_2(H_2O)]$	TC	4.1×10^4	0.82 ppm	H_2O	S27
$[Zn_3(L)_2(1,4\text{-}bimb)_3]_n$	TC	1.98×10^5	0.15 μM	H_2O	S28
$\{[Cd(2\text{-}F\text{-}tzba)(H_2O)]\cdot1.5H_2O\}_n$	TC	3.680×10^4	8.97 μM	H_2O	S29
	CTC	1.794×10^4	18.39 μM		
$\{[Cd(3\text{-}F\text{-}tzba)(H_2O)]\cdot1.5H_2O\}_n$	TC	3.514×10^4	9.39 μM		
	CTC	1.711×10^4	19.29 μM		
JNU-206-Eu	TC	2.37×10^4	0.36 μM	H_2O	S30
	CTC	1.33×10^4	0.62 μM		
$\{[Tb(\mu_6\text{-}Hcaa)(H_2O)]Cl\}_n$	TC	7.12×10^4	0.25 μM	H_2O	S31
	CTC	7.51×10^4	0.24 μM	H_2O	
$[Cd(bbimc)(ata)]_n$	**TC**	**7.22×10^4**	**0.208 μM**	**H_2O**	**this work**
	CTC	**4.45×10^4**	**0.307 μM**	H_2O	

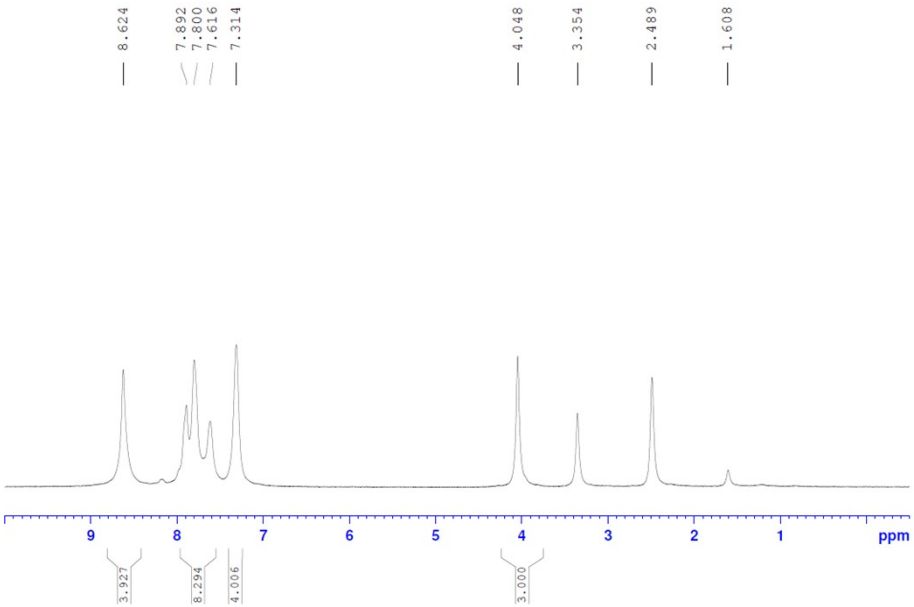

Fig. S1 ^{1}H NMR spectrum of bbimc in DMSO-d_6

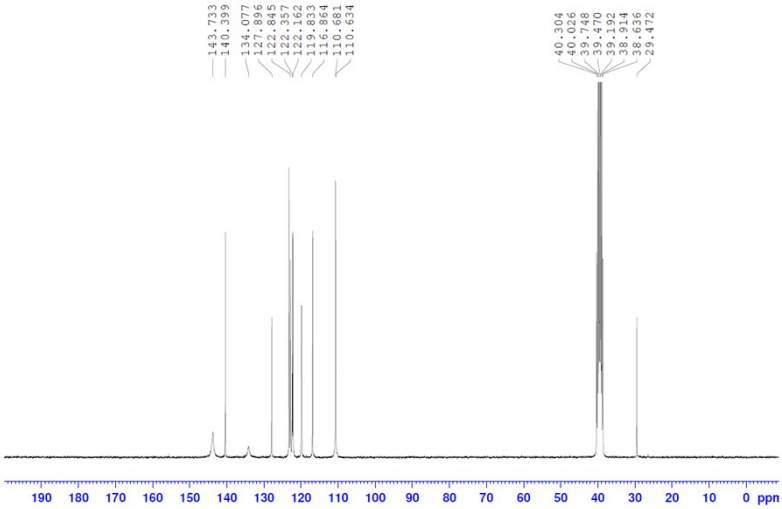

Fig. S2 ^{13}C NMR spectrum of bbimc in DMSO-d_6

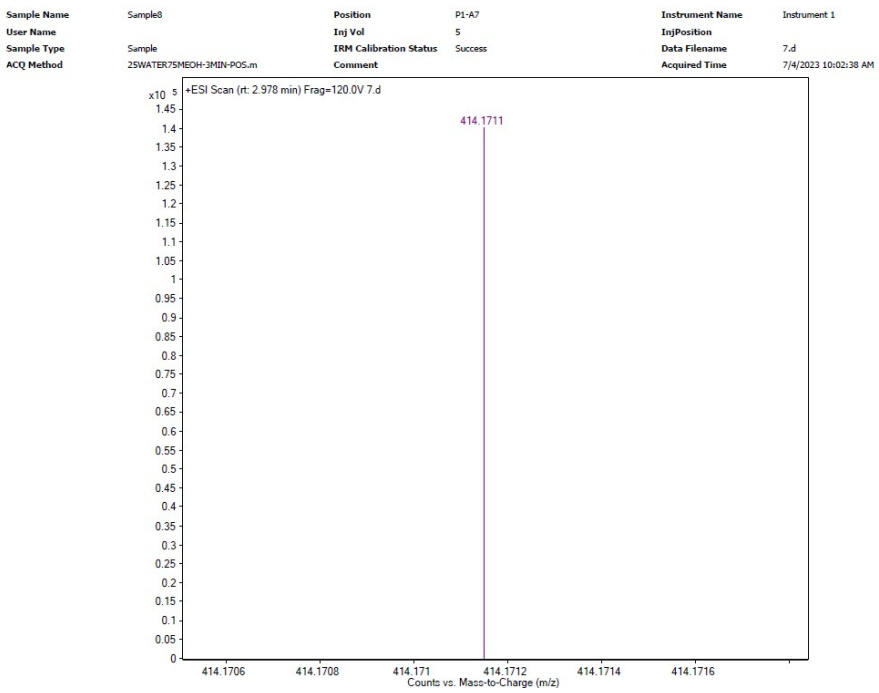

Fig. S3. HRMS of bbimc

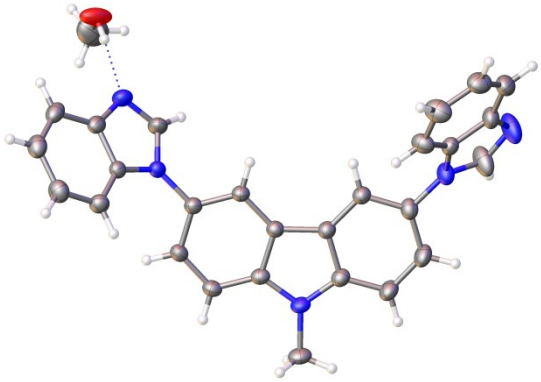

Fig S4 The molecular structure of bbimc

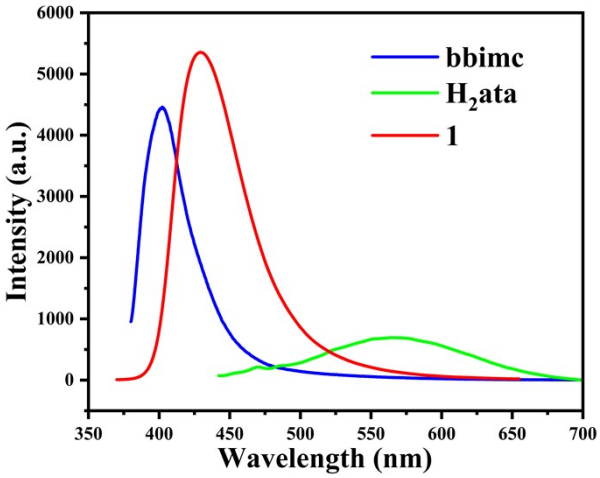

Fig. S5 Fluorescent emission spectra of the ligands and **1** in solid state at room temperature

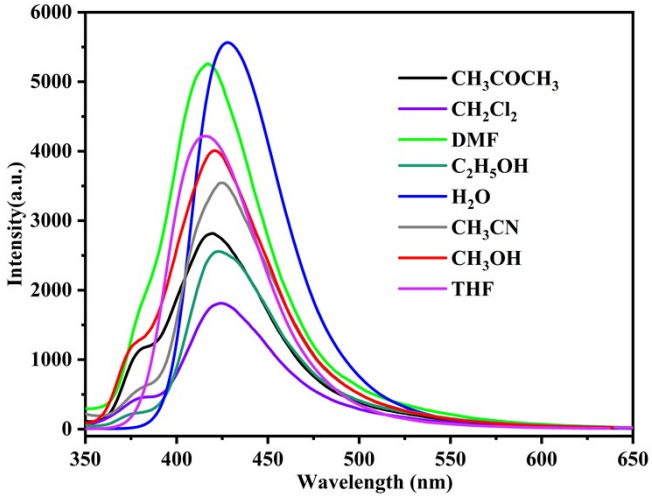

Fig S6 Emission spectra of CP **1** (2 mg) dispersed in the different organic solvents (2mL)

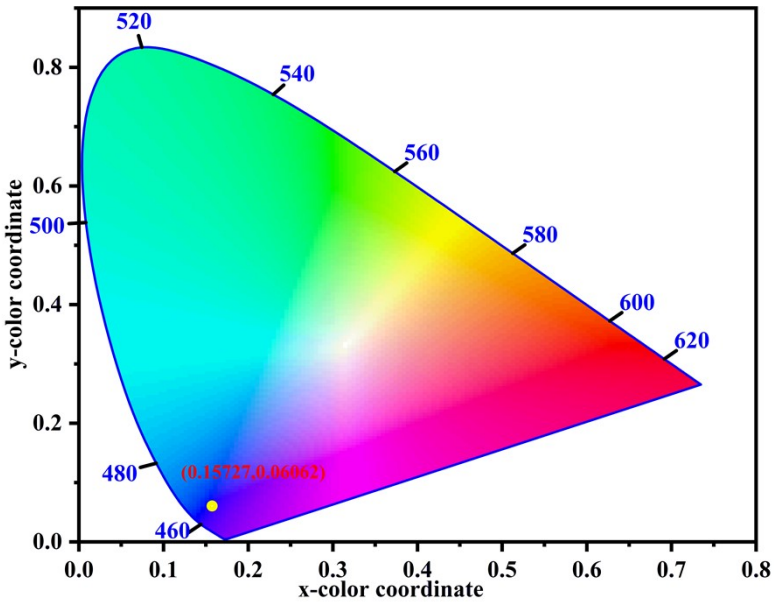

Fig. S7 CIE coordinate of **1**

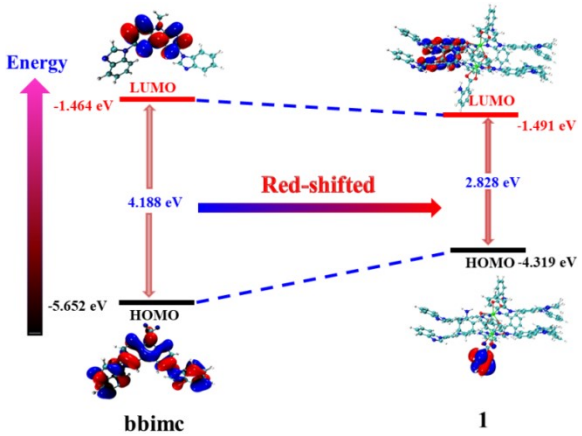

Fig. S8 The HOMO–LUMO energy levels of **1** and bbimc

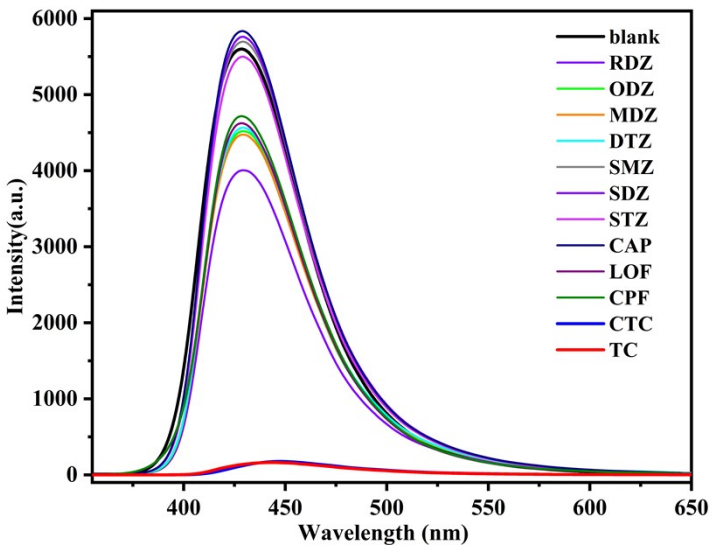

Fig. S9 Emission spectra of **1** dispersed in H_2O with the addition of different antibiotics

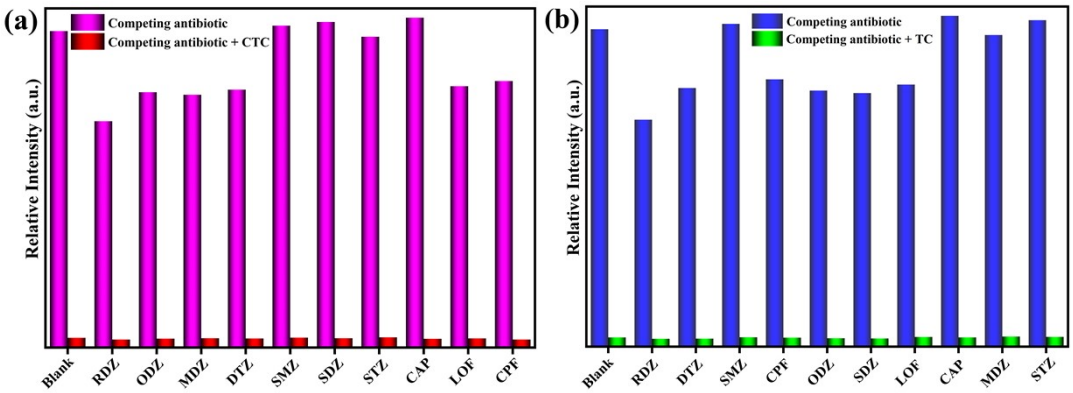

Fig. S10 Luminescence intensities of **1** before and after the addition of 0.2 mM CTC (a) or 0.2 mM TC (b) with the existence of mixed antibiotics (0.2 mM)

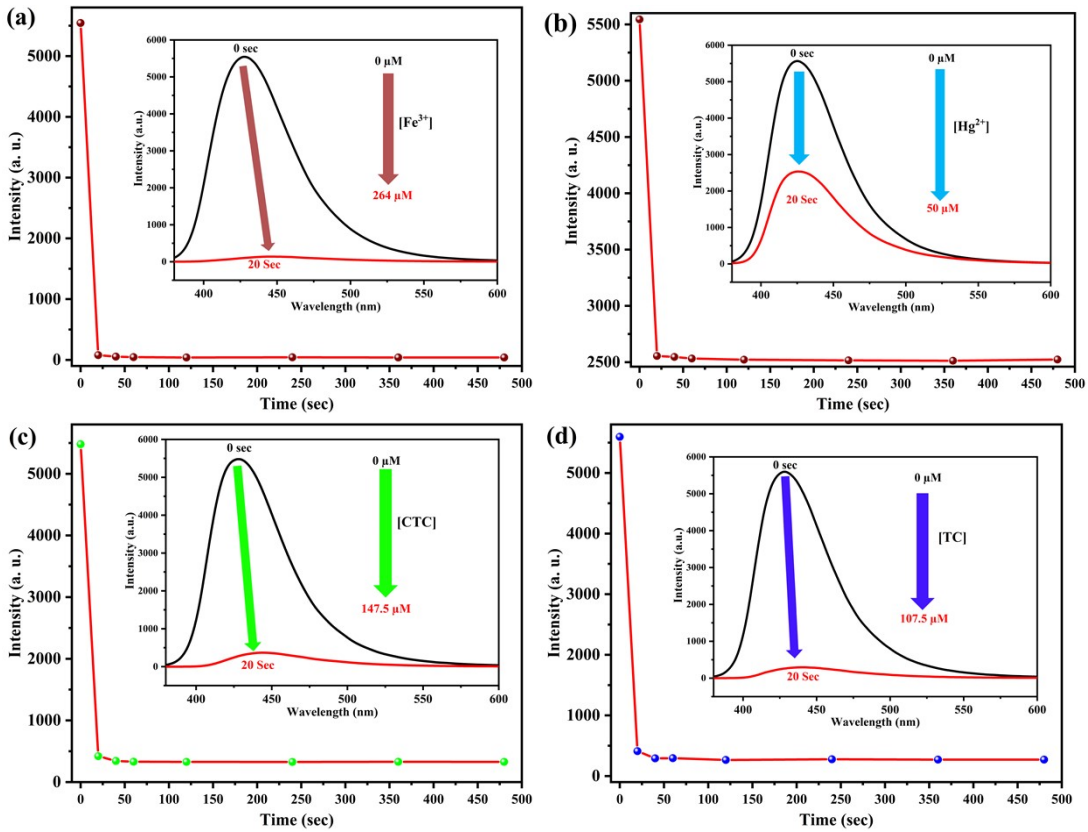

Fig. S11 Luminescence response time of **1** after the addition of Fe^{3+} (a), Hg^{2+} (b), CTC (c) and TC (d)

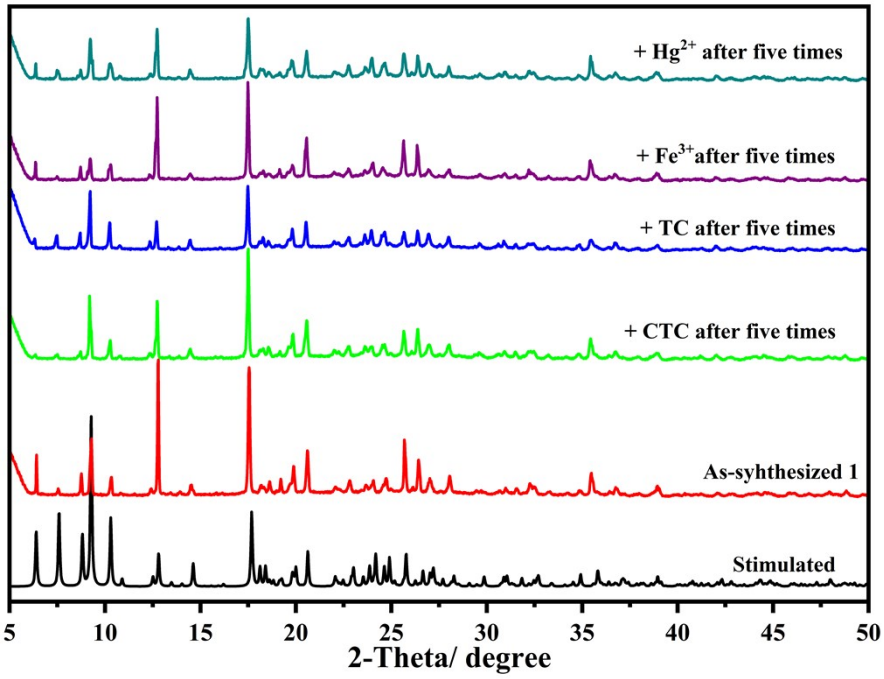

Fig. S12 The simulated and experimental PXRD patterns of **1** after sensing Hg^{2+}, Fe^{3+}, TC and CTC for 5 cycles

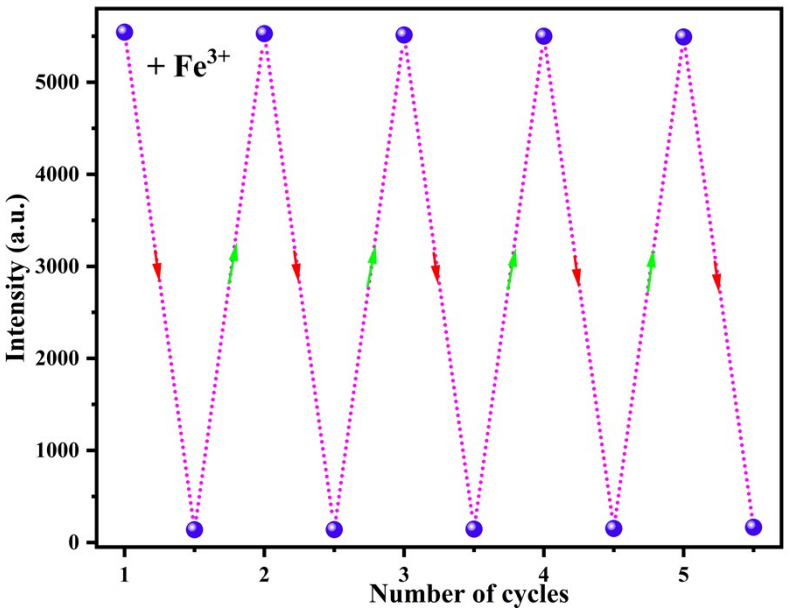

Fig. S13 Emission intensities of **1** toward Fe^{3+} after five cycles

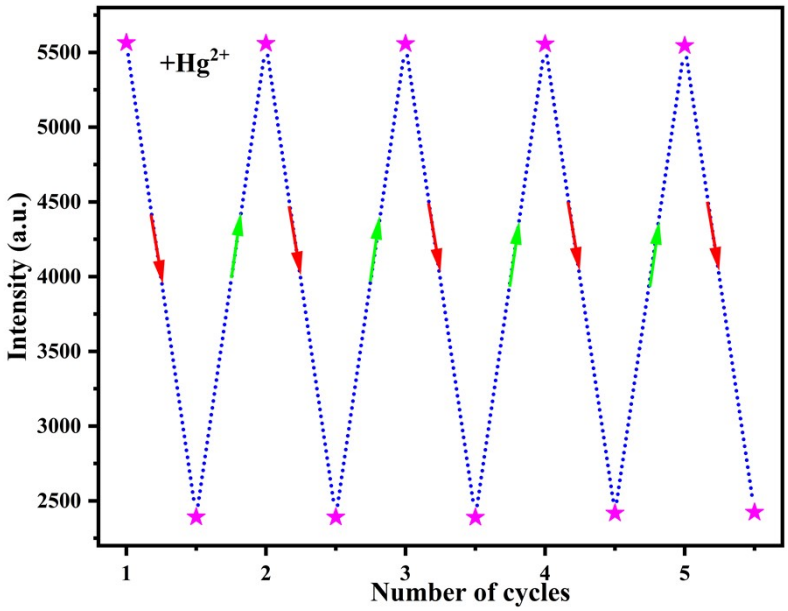

Fig. S14 Emission intensities of **1** toward Hg^{2+} after five cycles

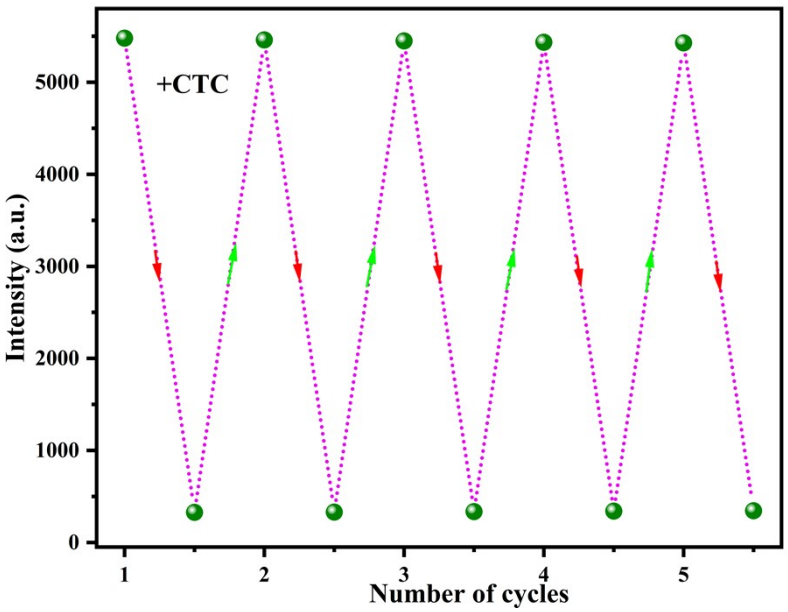

Fig. S15 Emission intensities of **1** toward CTC after five cycles

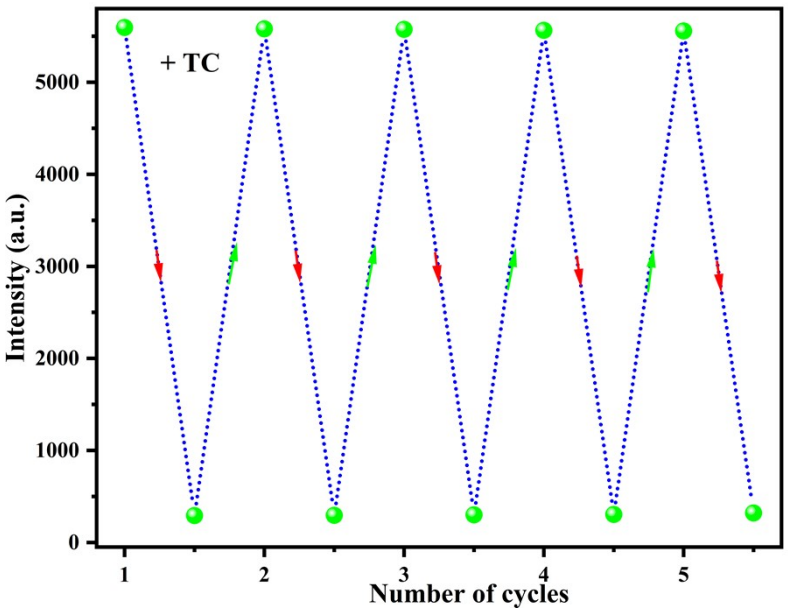

Fig. S16 Emission intensities of **1** toward TC after five cycles

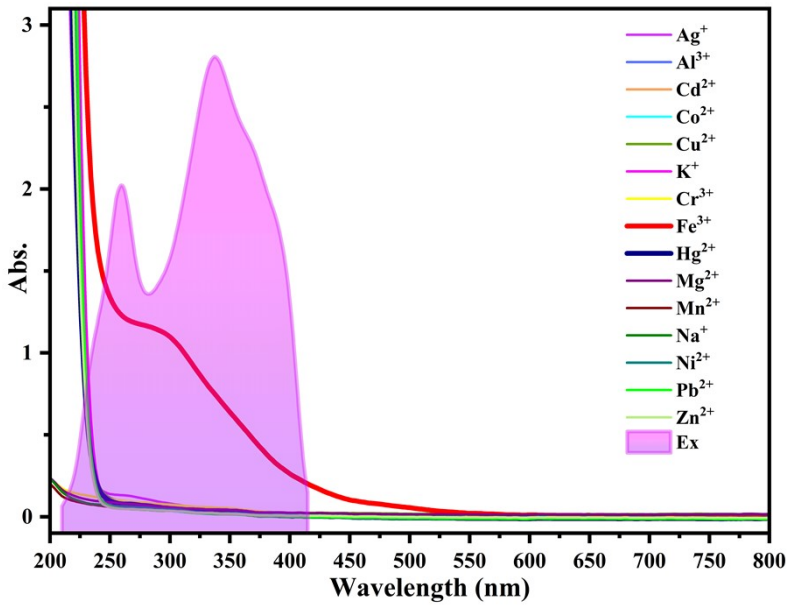

Fig. S17 The absorption spectra of cations and the excitation spectrum of **1**

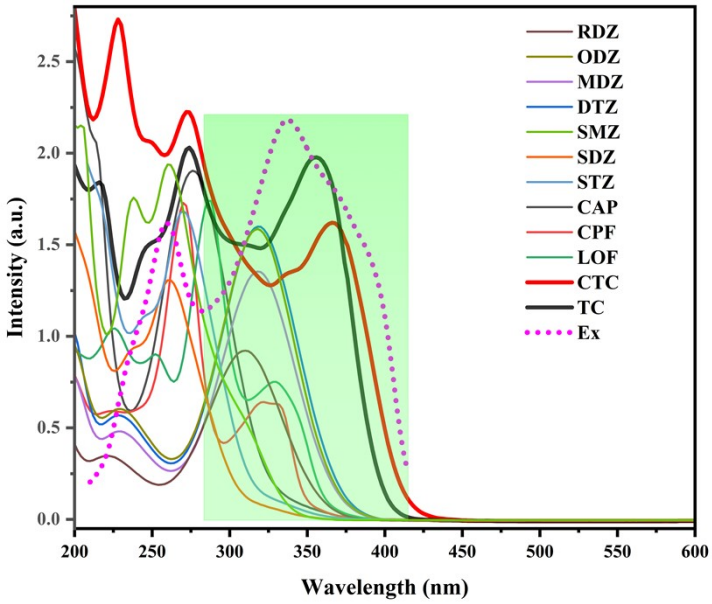

Fig. S18 Overlap between the absorption spectra of various antibiotics and the excitation spectrum of **1**

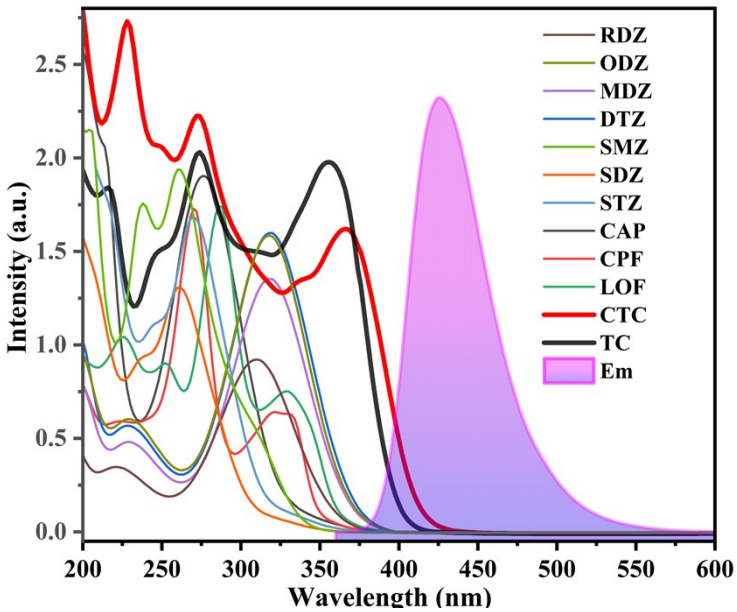

Fig. S19 Overlap between the absorption spectra of various antibiotics and the emission spectrum of **1**

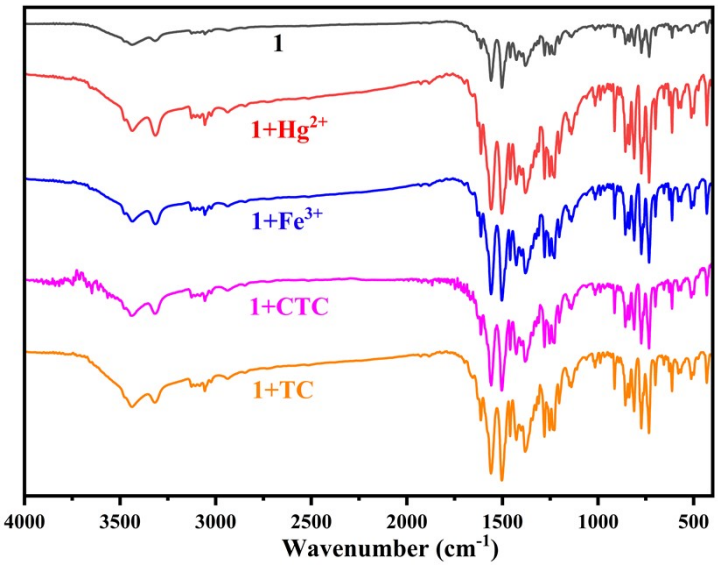

Fig. S20 IR spectra of **1** after sensing different analytes at room temperature

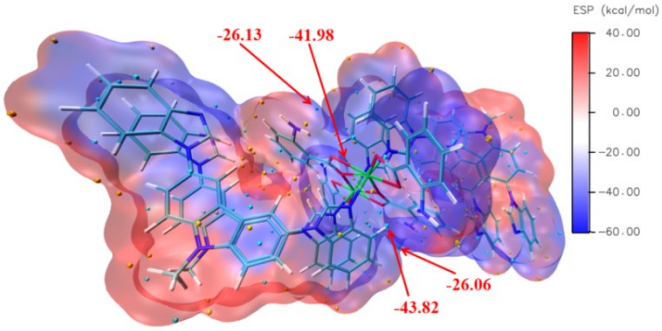

Fig. 21 Electrostatic surface potential of **1**, and the local minima and maxima of ESP are presented as bure and orange spheres, respectively

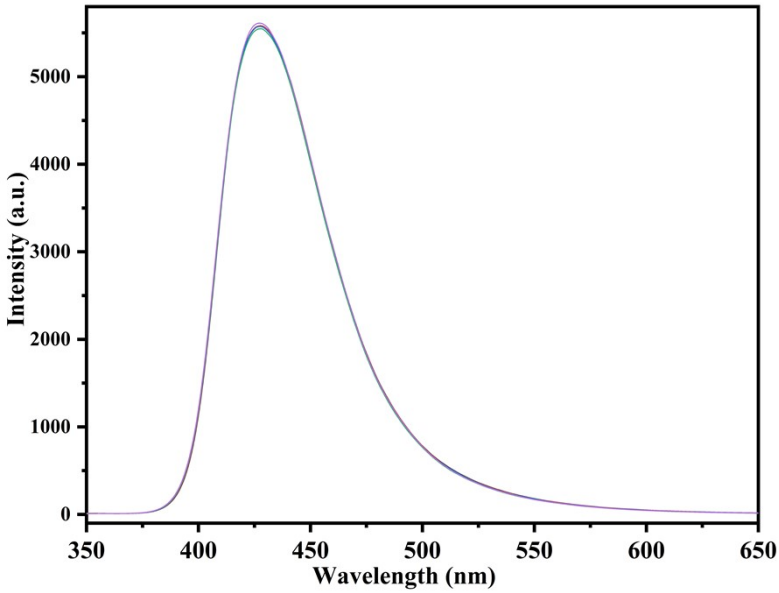

Fig. S22 The fluorescence spectra of blank 1 (1 mg·mL^{-1}) at 5 measurements (N = 5)

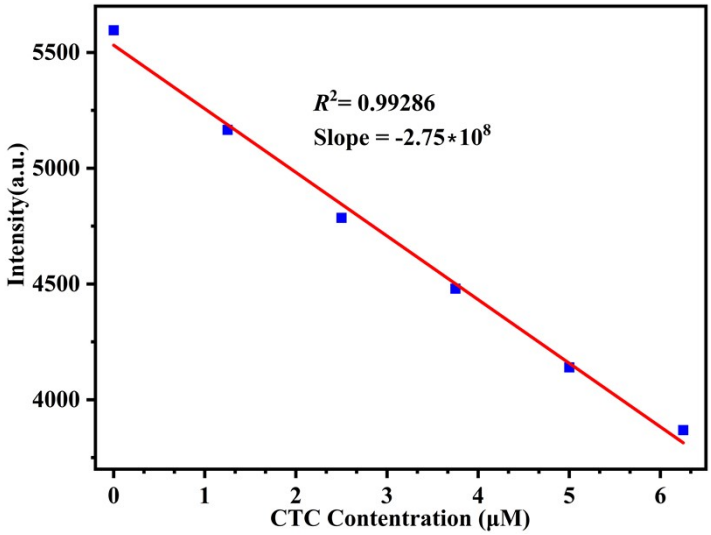

Fig. S23 The fitting curve of the luminescence intensity of **1** at different CTC concentration

LOD = 3σ/k

k = -2.75×108 M^{-1}

σ = 19.1 (N = 5)

Limit detection = 3σ/Slope = 0.208 μM

Reference

S1. SAINT, Version 6.02a, Bruker AXS Inc, Madison, WI, 2002.

S2. G. M. Sheldrick, SHELXT-Integrated Space-Group andCrystal-Structure Determination, Acta Crystallogr., Sect. A: *Found. Adv.*, 2015, **71**, 3-8.

S3. 37 G. M. Sheldrick, Crystal Structure Refinement with SHELXL, Acta Crystallogr., Sect. C: *Struct. Chem.*, 2015, **71**, 3-8.

S4. O. V. Dolomanov, L. J. Bourhis, R. J. Gildea, J. A. K. Howard and H. Puschmann, OLEX2: a Complete Structure Solution, Refinement and Analysis Program, J. Appl. Crystallogr., 2009, 42, 339-341.

S5. M. Y. Zhang, F. Y. Yi, L. J. Liu, G. P. Yan, H. Liu and J. F. Guo, *Dalton Trans.*, 2021, **50**, 15593-15601.

S6. S.-L. Yao, Y.-C. Xiong, X.-M. Tian, S.-J. Liu, H. Xu, T.-F. Zheng, J.-L. Chen and H.-R. Wen, *CrystEngComm*, 2021, **23**, 1898-1905.

S7. X.-K. Yang, W.-T. Lee, J.-H. Hu and J.-D. Chen, *CrystEngComm*, 2021, **23**, 4486-4493.

S8. F.-Y. Ge, G.-H. Sun, L. Meng, S.-S. Ren and H.-G. Zheng, *Cryst. Growth Des.,* 2019, **20**, 1898-1904.

S9. L. Deng, Y. Zhang, D. Zhang, S. Jiao, J. Xu, K. Liu and L. Wang, *CrystEngComm*, 2019, **21**, 6056-6062.

S10. H.-H. Yu, J.-Q. Chi, Z.-M. Su, X. Li, J. Sun, C. Zhou, X.-L. Hu and Q. Liu, *CrystEngComm*, 2020, **22**, 3638-3643.

S11. H. Zhang, Z.-J. Ding, Y.-H. Luo, W.-Y. Geng, Z.-X. Wang and D.-E. Zhang, *CrystEngComm*, 2022, **24**, 667-673.

S12. L.-N. Wang, Y.-H. Zhang, S. Jiang and Z.-Z. Liu, *CrystEngComm*, 2019, **21**, 4557-4567.

S13. X. Mi, D. Sheng, Y. Yu, Y. Wang, L. Zhao, J. Lu, Y. Li, D. Li, J. Dou, J. Duan and S. Wang, *ACS Appl. Mater. Interfaces*, 2019, **11**, 7914-7926.

S14. Y. Rachuri, B. Parmar, K. K. Bisht and E. Suresh, *Crystal Growth & Design*, 2017, **17**, 1363-1372.

S15. S. Khan, P. Das and S. K. Mandal, *Inorg. Chem.*, 2020, **59**, 4588-4600.

S16. T. Xia, T. Song, G. Zhang, Y. Cui, Y. Yang, Z. Wang and G. Qian, *Chemistry A European journal* **2016,** *22* (51), 18429-18434.

S17. K. Manna and S. Natarajan, *Inorg Chem*, 2023, **62**, 508-519.

S18. P. Wu, Y. Liu, Y. Liu, J. Wang, Y. Li, W. Liu and J. Wang, *Inorg Chem*, 2015, **54**, 11046-11048.

S19. Z. Xiaoxiong, Z. Wenjun, L. Cuiliu, Q. Xiaohong and Z. Chengyu, *Inorg Chem*, 2019, **58**, 3910-3915.

S20. L. Wen, X. Zheng, K. Lv, C. Wang and X. Xu, *Inorg Chem*, 2015, **54**, 7133-7135.

S21. X. Q. Cao, W. P. Wu, Q. Li, T. F. Zheng, Y. Q. Chen, J. L. Chen, S. J. Liu and H. R. Wen, *Dalton Trans*, 2023, **52**, 652-658.

S22. H. Zhu, C. Han, Y.-H. Li and G.-H. Cui, *Journal of Solid State Chemistry*, 2020, **282**.121132.

S23. Z. J. Wang, F. Y. Ge, G. H. Sun and H. G. Zheng, *Dalton Trans*, 2018, **47**, 8257-8263.

S24. F. Li, Y.-S. Hong, K.-X. Zuo, Q. Sun and E.-Q. Gao, *Journal of Solid State Chemistry*, 2019, **270**, 509-515.

S25. G.-N. Liu, R.-Y. Zhao, R.-D. Xu, X. Zhang, X.-N. Tang, Q.-J. Dan, Y.-W. Wei, Y.-Y. Tu, Q.-B. Bo and C. Li, *Crystal Growth & Design*, 2018, **18**, 5441-5448.

S26. G.-N. Liu, R.-D. Xu, R.-Y. Zhao, Y. Sun, Q.-B. Bo, Z.-Y. Duan, Y.-H. Li, Y.-Y. Wang, Q. Wu and C. Li, *ACS Sustainable Chemistry & Engineering*, 2019, **7**, 18863-18873.

S27. Q.-L. Cao, R.-T. Wang, J.-Y. Duan and G.-Y. Dong, *Journal of Solid State Chemistry*, 2022, **307**.

S28. L. Wang, W. Xu, W. Y. Li, M. Xie and Y. Q. Zheng, *Chem Asian J*, 2019, **14**, 4246-4254.

S29. H.-H. Wang, Y. Zhang, D.-B. Yang, L. Hou, Z.-Y. Li and Y.-Y. Wang, *Crystal Growth & Design*, 2021, **21**, 2488-2497.

S30. K. Wu, X.-Y. Liu, Y.-L. Huang, M. Xie, X. Xiong, J. Zheng, W. Lu and D. Li, *Inorganic Chemistry Frontiers*, 2022, **9**, 1714-1721.

S31. Y. Zhang, A. Wang, S. Feng, C. Yuan and L. Lu, *Dalton Trans*, 2023, **52**, 5243-5251.